8. Conference on the application of accelerators in research and industry
Denton, TX (USA) 12-14 Nov 1984
CEA-CONF--7741

Partial Kerma Factors for Neutron Interactions with ^{12}C at $20 < E_n < 65$ MeV *

R.W. Finlay, Ali S. Meigooni and J.S. Petler

Ohio University, Athens, Ohio 45701 U.S.A.

and

J.P. Delaroche †

Centre d'Etude de Bruyères-le-Chatel, B.P. No. 12

91680 Bruyères-le-Chatel, France

ABSTRACT

New measurements of elastic and inelastic scattering of 20-26 MeV neutrons from ^{12}C are presented and analyzed in terms of a deformed optical model potential. Results of these analyses have been compared with other recent differential and total neutron scattering measurements and with proton scattering data in order to develop a consistent representation of the energy dependence of the $n-^{12}C$ interaction over a broad energy range. Applications of the data and the model to problems in neutron dosimetry are discussed.

---

* This investigation was supported by PHS Grant Number CA-25193 awarded by the National Cancer Institute, DHHS.

† Supported in part by the National Science Foundation.

1. Introduction

The introduction of clinical neutron radiotherapy facilities that produce a substantial flux of neutrons with energy greater than 20 MeV has focussed much attention on the general problem of neutron dosimetry in this energy region. Early efforts to tabulate kerma factors for neutrons incident on carbon, oxygen, etc. were hindered by the near-total lack of the relevant neutron cross section data. Recently, much effort has gone into the application of nuclear reaction theory in order to calculate the required, but unmeasured, cross sections, and a few important experiments have been performed that provide crucial tests for these calculations. Most of the attention has been placed on the calculation and measurement of charged-particle-production cross sections. The present work deals with the scattering of neutrons by nuclei and the contributions that these measurements can make to our understanding of neutron dosimetry.

Compared with the difficulties involved in the measurement of (n,xp) and (n,xα) reactions, neutron scattering experiments are relatively straightforward and can be performed with good accuracy. The framework for theoretical interpretation of the data--the optical potential model--is very well established for heavy nuclei and can be successfully applied to the light nuclei of interest in dosimetry provided that a large enough base of high quality data is available. Measurement of differential elastic scattering cross sections over a wide angular range provides a reliable determination of the reaction cross section at that energy since $\sigma_{reaction} = \sigma_{total} - \sigma_{elastic}$, and σ_{total} is well known. Simultaneous measurement of inelastic scattering is also important since any of the non-elastic neutron

flux that goes into inelastic scattering to particle-stable states is not available for reaction channels such as (n,xp), (n,xα), etc. Moreover, measurement of differential cross sections for elastic and inelastic scattering provides detailed information about the heavy-ion-recoil contribution to kerma. This information is useful in the interpretation of the very high LET($\sim 10^3$ kev/μ) region of microdosimetric spectra. Finally, the decay of a highly excited nuclear state is not entirely independent of its formation; thus, the population of excited states by inelastic neutron scattering can be related to the emission of charged particles when these states decay.

2. Experimental Methods

The Ohio University beam swinger facility [1] provides the opportunity to measure low background, high resolution neutron time-of-flight spectra. Neutrons in the energy range 18-26 MeV are produced with the $T(d,n)^4He$ reaction and are detected--after scattering from the sample of interest--by an array of seven large NE213 liquid scintillation counters positioned in a long, well-collimated time-of-flight tunnel. In the beam swinger geometry, angular distributions are measured by varying the direction of the incident deuteron beam through mechanical rotation of the swinger magnet. This arrangement has the significant advantage that the detectors and collimator are fixed in space thus permitting massive, fixed shielding arrangements.

Scattering samples are typically right circular cylinders approximately 2 cm in length and diameter. Time-of-flight spectra are taken over the widest possible angular range ($\sim 10°$-$160°$) both with the sample in

position and with the scattering sample removed (background). Raw data are corrected for a variety of effects including multiple scattering, flux attenuation, energy-dependent detector efficiency, and finite angular geometry. Cross sections are normalized by measuring the ratio of detector counting rate to monitor counting rate at 0° with the scattering sample removed.

This facility has been used to measure differential elastic and inelastic scattering cross sections for 18-26 MeV neutrons incident on C, N O and Ca (plus several other target nuclei of less interest in dosimetry). The remainder of the discussion will be focussed primarily on the ^{12}C nucleus since analysis of these data is essentially complete. A preliminary report of this work, which dealt only with the ground state rotational band of this permanently deformed nucleus, has been published [2]. A more complete analysis including scattering to other excited states has been submitted for publication [3].

3. Analysis

Elastic scattering of fast neutrons from nuclei can be described in the framework of an optical model in which the interaction between an incident neutron and the nucleus can be represented by a complex potential:

$$V(r) = -V_R\, f(r,R_R,a_R) - iW_V f(r,R_I,a_I) + 4i\, W_D a_I \frac{d}{dr}\left(f(r,R_I,a_I)\right)$$

$$+ \left(\frac{\hbar}{mc}\right)^2 \left(V_{so}\, \frac{1}{r}\, \frac{d}{dr}\left(f(r,R_{so},a_{so})\right)\right) \vec{L} \cdot \vec{\sigma}$$

where

$$f(r,R_i,a_i) = \frac{1}{1 + \exp[(r-R_i)/a_i]} ; \qquad R_i = r_i A^{1/3}.$$

For a deformed nucleus such as ^{12}C the R_i are potential radii which describe the collective motion of the nuclear surface. For the ground state rotational band, the R_i describe an oblate nuclear surface with quadrupole and hexadecapole deformations. Other excited states in ^{12}C are described as octupole vibrations, beta vibrations diffuseneess oscillations, etc. of the deformed nuclear surface (the rotation-vibration model). Since the static deformation of ^{12}C is quite large ($\beta_2 = -0.6$), elastic and inelastic scattering channels are strongly coupled, so all scattering calculations were performed with the coupled channel code ECIS79 [4]. New formalisms were developed in order to calculate the effects of potential depth and diffuseness oscillations around an equilibrium shape with permanent deformation [5].

An illustration of the success of the deformed potential model is given in fig. 1 where the calculations for elastic scattering are compared with the data for 20-26 MeV neutrons (present work) and 40 MeV neutrons [6]. The energy dependences of the neutron optical potential parameters are given in table 1. It was shown in ref. 2 that this deformed potential model provides a good description of the neutron total cross section and reaction cross section from 20 to 100 MeV. The parameters in table 1 differ slightly from those given in ref. 2: in the present work β_4 was reduced and β_2 slightly increased as suggested by De Leo et al. [7]. W_D was adjusted to compensate for these changes. Predictions for the total and reaction cross sections are essentially the same for both potentials.

It should be emphasized that the potential parameters of table 1 are intended to describe the $n+^{12}C$ interaction for $20 < E_n < 100$ MeV. Below 20 MeV, this interaction is characterized by many strong resonances, and the optical model can be expected, at best, to give only a rough representation of average scattering properties.

One other improvement over the work of ref. 2 should be mentioned. In that report, only the ground state rotational band was considered and the calculations were performed with a coupling scheme that included the ground state, the 2^+ state at 4.44 MeV and the 4^+ state at 14.1 MeV. More recently the calculations were expanded and the 3^- state at 9.64 MeV was included in the coupling scheme [3]. The effect of this change was to improve the fit to the 2^+ differential cross section at large angles and, consequently, to bring the model predictions for recoil kerma for this state into better agreement with the experimental values. Above 30 MeV, the results were essentially unchanged from ref. 2. Table 2 contains the revised results.

The neutron optical potential can be transformed into a proton optical potential by the addition of a real Coulomb correction term given by [8]

$$\Delta V_c = 0.46\ Z/A^{1/3}\ (\text{MeV}).$$

With no further changes in the parameters of table 1, the model gives an excellent description of proton elastic scattering from 30 to 65 MeV and a description of proton inelastic scattering in this region that is generally quite satisfactory. Fits to the proton data were not improved by the inclusion of an imaginary Coulomb correction, so this term was omitted. Details of the analysis are presented in ref. 3.

4. Inelastic Scattering and the $^{12}C(n,n')3\alpha$ Reaction

With the exception of the 2^+ state at 4.44 MeV, all of the collective states in ^{12}C populated in inelastic scattering can decay, in one or more steps, into three alpha particles. For $E_n > 20$ MeV, the largest contribution to kerma for ^{12}C comes from these alpha particles so it is important to consider this process in some detail. In a recent nuclear emulsion experiment, Antolković et al. [9] measured the total cross section for $^{12}C(n,n')3\alpha$ from threshold to 35 MeV. In that kinematically complete experiment, it was possible to determine the partial cross section for 3α events resulting from the decay of the 9.64 MeV state in ^{12}C. In the present experiment, the cross section for formation of this state by inelastic scattering is directly determined. Since the 9.64 MeV state decays over 99% of the time into three alpha particles, these two cross sections should be directly comparable.

Results for inelastic scattering of 20-26 MeV neutrons to the 9.64 MeV state are shown in fig. 2. The solid lines represent Legendre polynomial fits to the data, and the dot-dash lines are the results of coupled-channel calculations for which the state is assumed to be the head of a $K^\pi = 3^-$ octupole vibrational band. The rapid changes in shape of the differential cross section for this state between 20 and 26 MeV might be evidence for some resonance phenomena in the exit channel. Even so, the model provides a fairly good description of the data especially at 26 MeV. The Coulomb-corrected potential gives a very good description of proton inelastic scattering [7,10,11] to this state in the range $30 < E_p < 65$ MeV (fig. 3).

The comparison of proton scattering, neutron scattering, nuclear emulsion experiments, and model calculations is shown in fig. 4. Diamonds are the data of Antolković et al. [9], filled circles and squares are the angle-integrated cross sections from neutron and proton scattering, respectively, and the solid line is the prediction from the deformed potential model (table 1) with constant vibration amplitude. Although some of the specific fluctuations in the Antolković et al. data are not confirmed by the scattering data, it seems clear that the scattering data and the deformed potential model calculation are in very good general agreement with the Antolković results.

The measurements of the $^{12}C(n,n')3\alpha$ cross section by Antolković et al. [9] have been recently reanalyzed by Brenner and Prael [12] who use the intranuclear cascade model with Fermi breakup (INC/FB) to simulate some of the effects that should be seen in the emulsion experiment. Brenner and Prael also calculate the partial cross section for the $^{12}C(n,n')^{12}C_{9.64}(3\alpha)$ reaction, and their results are shown as the dashed line in fig. 4. It would appear that the scattering data are in better agreement with the original Antolković results [9] than with this recent reevaluation [12]. To some extent, this last statement depends on the appropriateness of including (p,p') measurements in fig. 4. Since the Coulomb correction for protons on ^{12}C is only about 1.2 MeV, this inclusion seems to be valid. Moreover, the success of the deformed potential model in describing a broad range of neutron and proton scattering data [3] lends support to this approach.

4. Conclusions

Analysis of elastic and inelastic scattering of high energy neutrons from light nuclei in terms of an optical potential model has been successfully demonstrated in the case of ^{12}C. Similar work on ^{14}N, ^{16}O and ^{40}Ca is in progress. The contribution to kerma of recoiling target nuclei following elastic and inelastic scattering is measured at several energies and is in good agreement with the model predictions. Differential scattering cross sections can be transformed directly into recoil-ion energy spectra for comparison with microdosimetric spectra.

The study of the population and decay of the 3^- (9.64 MeV) state in ^{12}C demonstrates how the relatively high accuracy of neutron (and proton) scatttering experiments can be used to provide benchmarks for the much more difficult experimental problem of determining neutron-induced charged-particle production directly.

REFERENCES

1. R.W. Finlay, C.E. Brient, D.E. Carter, A. Marcinkowski, S. Mellema, G. Randers-Pehrson and J. Rapaport, Nucl. Instr. and Meth. 198 (1982) 197.

2. Ali S. Meigooni, J.S. Petler and R.W. Finlay, Phys. Med. Biol. 29 (1984) 643.

3. Ali S. Meigooni, R.W. Finlay, J.S. Petler and J.P. Delaroche, submitted to Nucl. Phys.

4. J. Raynal, code ECIS79 (unpublished).

5. J.P. Delaroche and A.S. Meigooni, submitted to Nucl. Phys.

6. R.P. DeVito, Ph.D. thesis, Michigan State University (1979), unpublished.

7. R. De Leo, G. D'Erasmo, A. Panteleo, M.N. Harakeh, E. Cereda, S. Micheletti and M. Pignanelli, Phys. Rev. C28 (1983) 1443.

8. J. Rapaport. J.D. Carlson, D. Bainum, T.S. Cheema and R.W. Finlay, Nucl. Phys. A286 (1977) 232.

9. B. Antolković, I. Šlaus, D. Plenković, P. Macq and J.P. Meulders, Nucl. Phys. A394 (1983) 87.

10. G.R. Satchler, Nucl. Phys. A100 (1967) 481; A100 (1967) 497.

11. S. Kato et al., Nucl. Instr. and Meth. 169 (1980) 589.

12. D.J. Brenner and R.E. Prael, Nucl. Sci. and Engr. 88 (1984) 97.

Table 1. Neutron Optical Potential (Eq. (1)) Parameters. Strengths and Incident Energies in MeV; Radii and Diffusenesses in fm. Relativistic Kinematics Used Throughout.

$$V(E) = 50.78 - 0.34\,E$$

$$W_V(E) = \begin{cases} 0 & , \quad E \leq 20 \text{ MeV} \\ 15.5\left[1 - \dfrac{2}{1 + \exp\left(\frac{E-20}{25}\right)}\right] & , \quad E > 20 \text{ MeV} \end{cases}$$

$$W_D(E) = \begin{cases} \exp(0.094\,E) & , \quad E \leq 21 \text{ MeV} \\ 10.29 - 0.145\,E & , \quad 21 \text{ MeV} \leq E < 71 \text{ MeV} \\ 0 & , \quad E \geq 71 \text{ MeV} \end{cases}$$

$V_{SO} = 6.20$

$r_V = 1.22$ $\qquad r_D = 1.25$ $\qquad r_{SO} = 1.05$

$a_V = 0.478 + 0.0043\,E$ $\qquad a_D = 0.27$ $\qquad a_{SO} = 0.55$

$\beta_2 = -0.61$, $\qquad \beta_4 = 0.05$

Table 2

KERMA FACTORS FOR ELASTICALLY AND INELASTICALLY RECOILING CARBON NUCLEI—MODEL PREDICTION

E_n (MeV)	Elastic (Gy m^2 x 10^{-15})	Inelastic (2^+, 4.44 MeV) (Gy m^2 x 10^{-15})
20	0.495	0.143
22	0.460	0.120
24	0.448	0.105
25	0.441	0.096
26	0.434	0.091
30	0.401	0.077
35	0.356	0.065
40	0.321	0.054
45	0.282	0.047
50	0.251	0.041
55	0.226	0.036
60	0.206	0.033
65	0.185	0.030

FIGURE CAPTIONS

Fig. 1 Elastic scattering of 20-40 MeV neutrons from ^{12}C. Solid lines are the results of calculations made with the deformed optical potential model of table 1.

Fig. 2 Inelastic neutron scattering to the 3^- state at 9.64 MeV in ^{12}C. Solid lines are fits to the data obtained from a Legendre polynomial expansion. Dash-dot lines are calculations made with the rotation-vibration model and the deformed optical potential.

Fig. 3 Inelastic proton scattering to the 3^- state at 9.64 MeV in ^{12}C. Solid lines are calculations made with the rotation-vibration model.

Fig. 4 Excitation function for the 3^- state in ^{12}C. ◇ : Antolković et al., ref. 9; ● : present work; ■ : proton scattering, refs. 7, 10, 11. The solid line is the prediction of the rotation-vibration model. The dashed curve shows the recommended values for this cross section by Brenner and Prael (ref. 12).

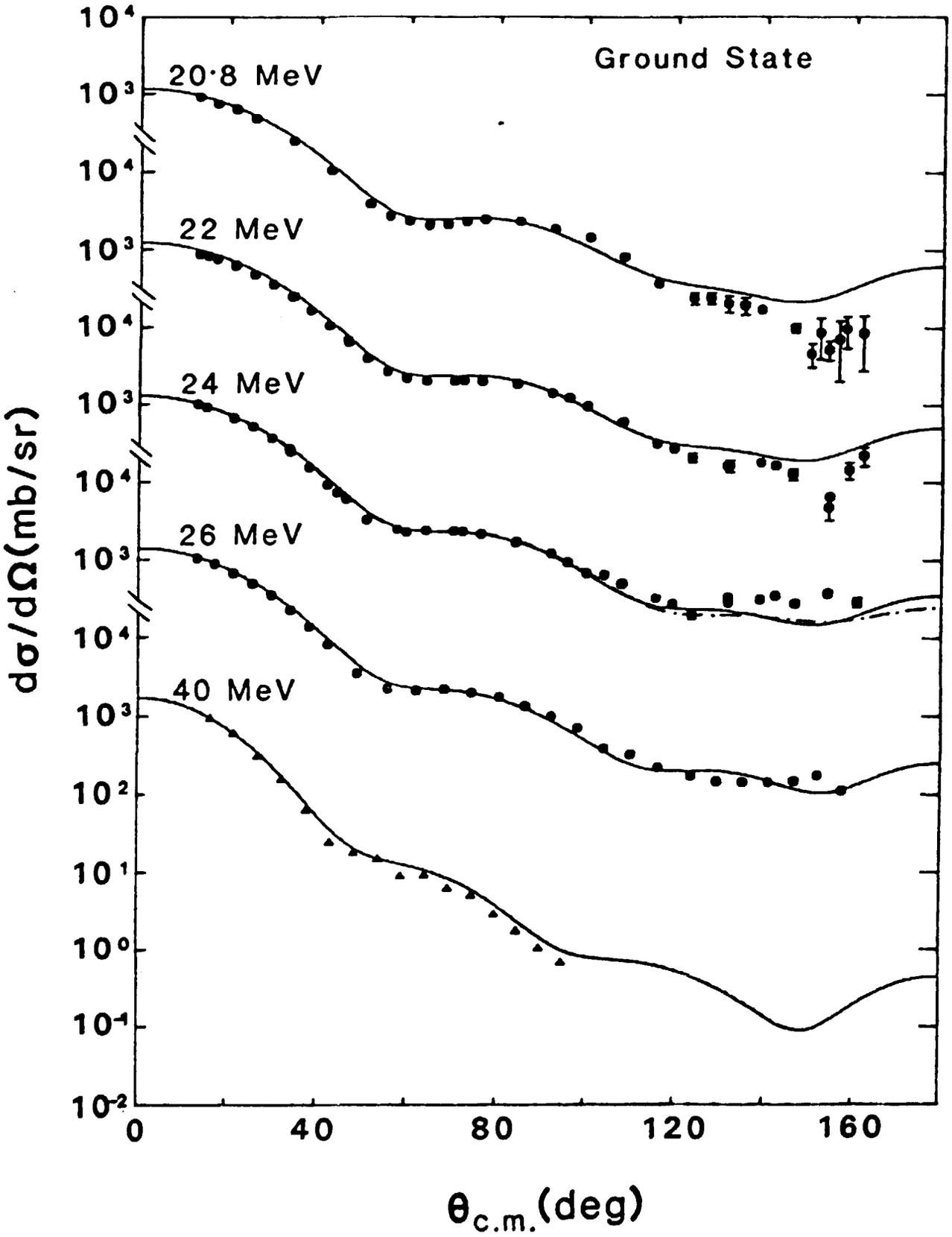
Ground State
20·8 MeV
22 MeV
24 MeV
26 MeV
40 MeV
dσ/dΩ(mb/sr)
θc.m.(deg)
0
40
80
120
160

FIGURE 1

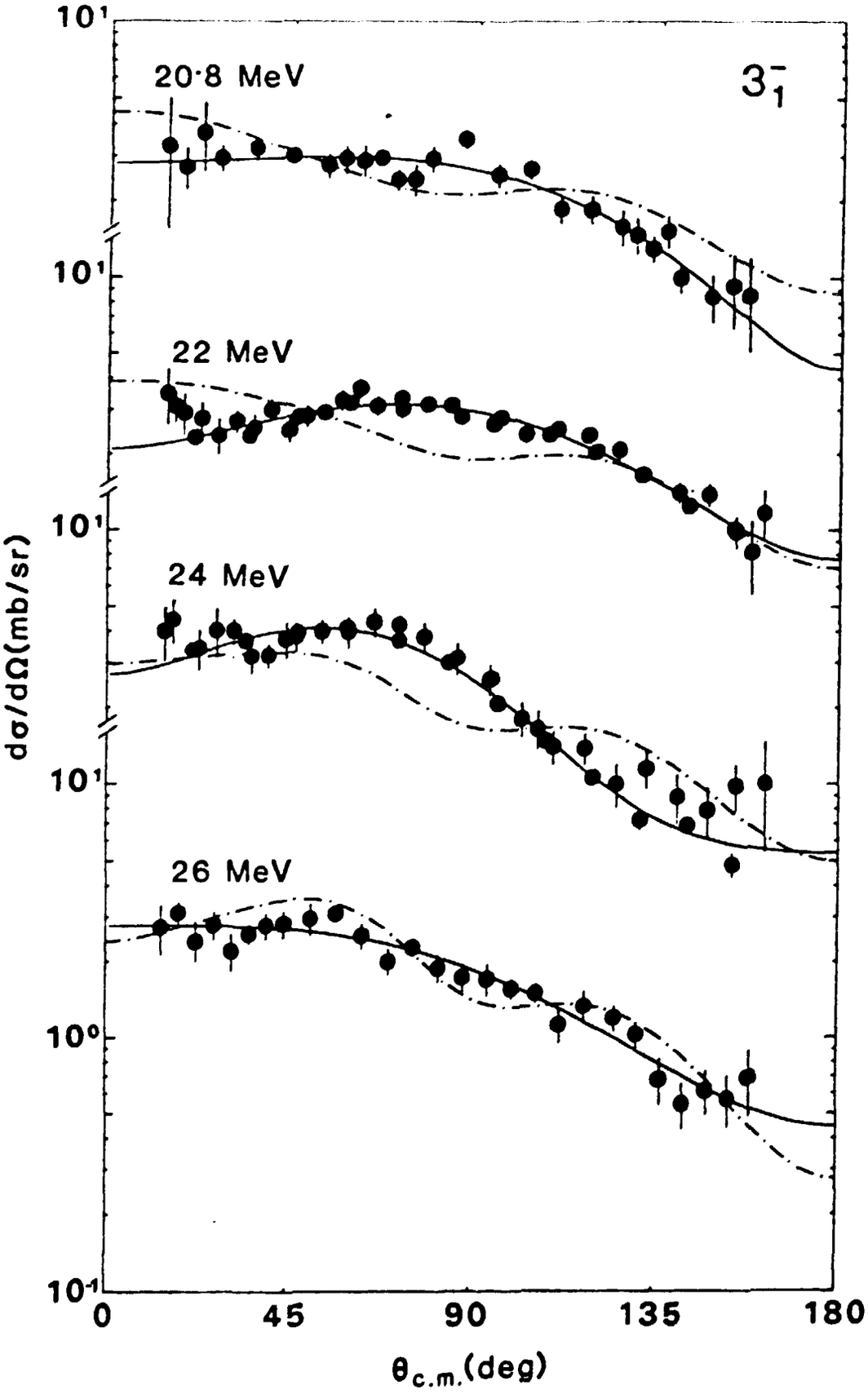
20·8 MeV
3_1^-
22 MeV
24 MeV
26 MeV
10^1
10^1
10^1
10^1
10^0
10^{-1}
dσ/dΩ(mb/sr)
0
45
90
135
180
$\theta_{c.m.}$(deg)

FIGURE 2

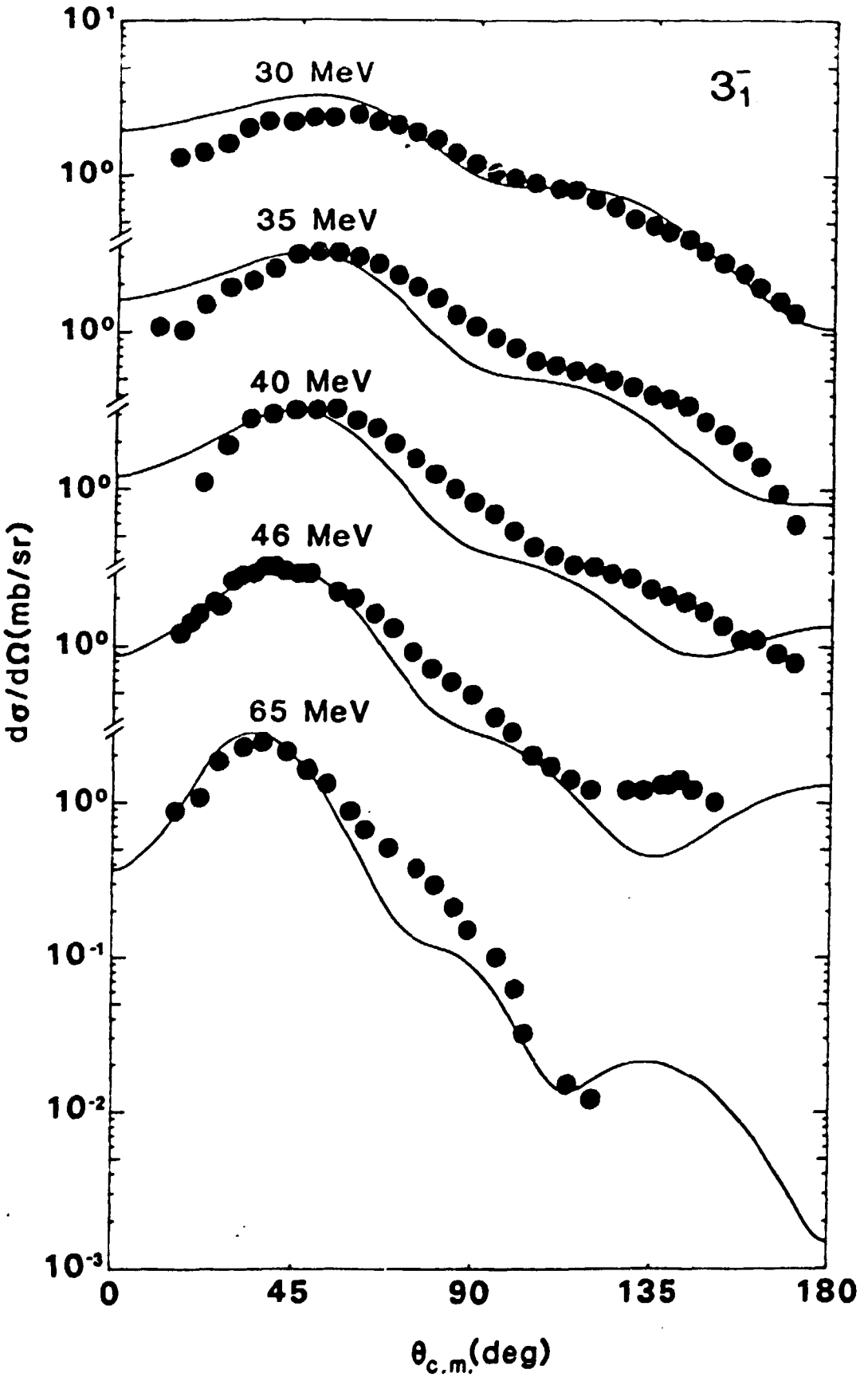
30 MeV
3_1^-
35 MeV
40 MeV
46 MeV
65 MeV
10^1
10^0
10^0
10^0
10^0
10^0
10^{-1}
10^{-2}
10^{-3}
$d\sigma/d\Omega$(mb/sr)
0
45
90
135
180
$\theta_{c.m.}$(deg)

FIGURE 3

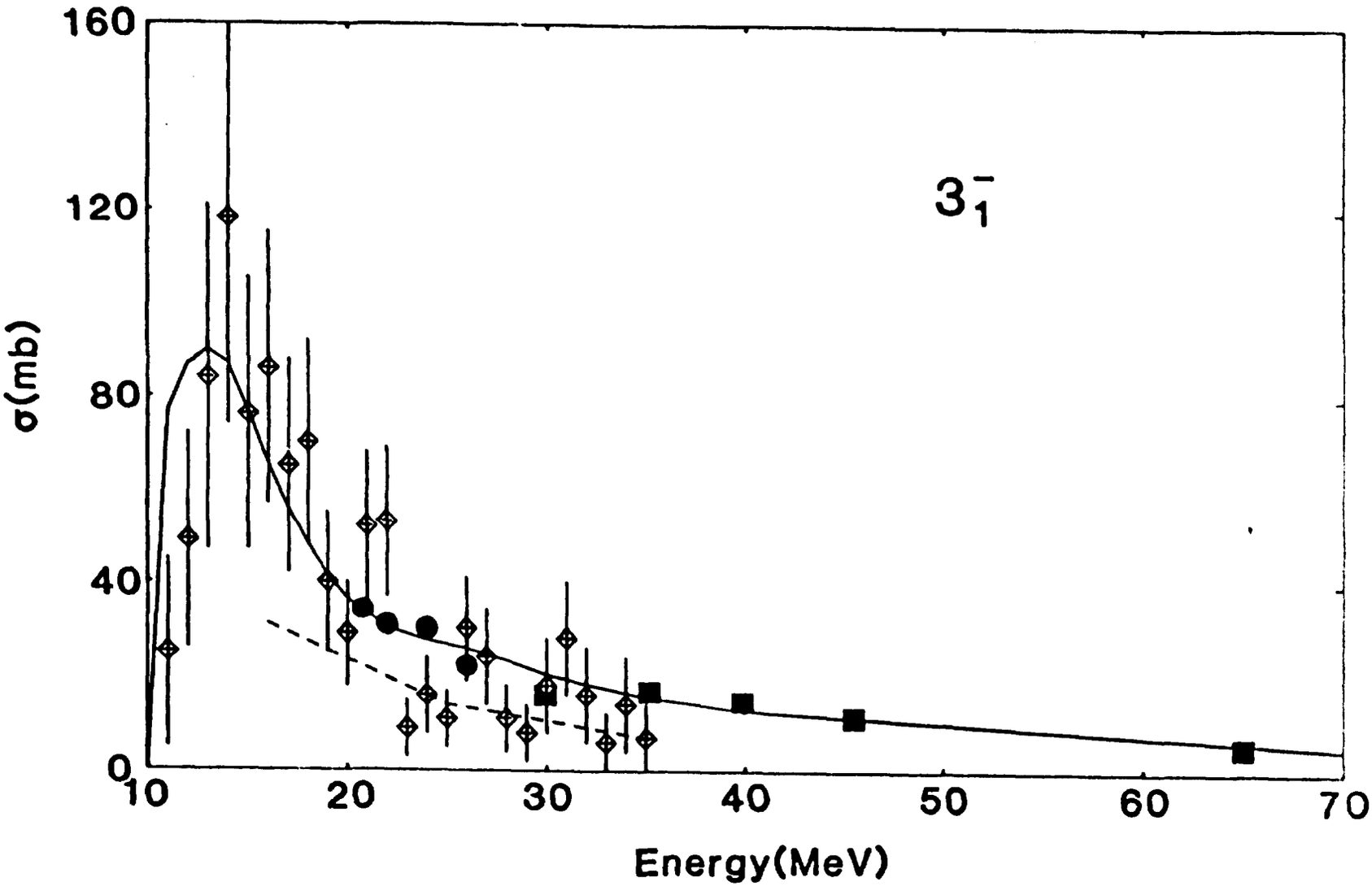

FIGURE 4